Advancements in Brushite cement formulations for bone repair

Morilla Espino, C.

Chapter 3: Synthesis and evaluation of a collagen–brushite cement as a drug delivery system.

This chapter is based on:

Morilla, C., Lima, Y. M., Fuentes, G., & Almirall, A. (2018). *International Journal of Materials Research*, *110*(4), 367-374.

Introduction

Calcium phosphates are well known biomaterials that promote bone regeneration and have excellent biocompatibility and bioactivity, which have caused a significant increase in their use in biomedical applications in recent years. These materials are used in various applications of orthopedic and maxillofacial surgery, either for filling bone defects, increase of the alveolar ridge, implants of the middle ear, fusion of spinal vertebrae or in the coating of metal prostheses. They are applied in different forms: as granulates, blocks of different shapes or as cements that solidify during their application [1]. The calcium phosphate cements (CPCs) have the advantage that they are prepared as a paste that sets in a few minutes and can easily adapt to the shape of the bone defect, which facilitates its application [2, 3]. These materials are used not only as dental cements, but also as bone reabsorbable implants. Particularly, and unlike other materials, these biomaterials can repair bone defects in a permanent way [4], promoting the formation of new bone tissue during the cement degradation [5] due to their osteoconductivity [6, 7]. In addition, the characteristics of calcium phosphate cements make them an excellent alternative for drugs release [8, 9].

Mirtchi and Lemaître described the brushite cements in 1989 [2, 10]. These materials are prepared by mixing water with a powder consisting of an acid calcium phosphate (monocalcium phosphate monohydrate, MCPM) and a basic calcium phosphate (β-tricalcium phosphate, β-TCP). The result of this mixture is a mouldable paste that solidifies by an exothermic reaction forming a hard material composed mainly of dicalcium phosphate dehydrate (DCPD), also known as brushite [4].

Subsequent studies showed that brushite cements are biocompatible; however, they are difficult to handle, harden too quickly (usually less than 30 s) and have poor mechanical properties. Several additives have been added to these cements to improve some of their properties: injectability [11], setting time [4], cohesion and mechanical properties [12]. The idea of using polymers to improve the mechanical properties of cements came from bone itself, which is a composite material made of an organic phase reinforced with hydroxyapatite crystals. Type I collagen is the main component in the organic phase of bone, and has a crucial role in the tensile strength of mineralized tissues [4], has been used as reinforcement for CPC [13] and promotes osteogenesis [14].

On the other hand, infection risk on surgical maxillofacial procedures requires the use of antibiotics, generally supplied in oral prescriptions in large quantities to ensure the appropriate therapeutic dosage on the treated site. A great number of bone implant infections are caused by

bacteria, which are very common in buccal cavity and are related to periodontal disease. Among other antibiotics, tetracycline is a well know an effective antibiotic with a broad- spectrum against bacterial infection, usually related to periodontal disease [15, 16].

In the present study, several brushite or DCPD bone cements for maxillofacial applications made from MCPM and *β*-TCP with or without collagen were prepared and evaluated as drug release systems for tetracycline. Although the use of CPCs as drug delivery system has been analysed, the study of more complex formulations that includes reinforcement materials, such as collagen, could have a significant impact on the development of more efficient bone regenerative biomaterials with the capability to be used as a drug delivery system.

Experimental procedure

Cements preparation

All chemicals employed were of analytical grade, used as received. *β*-TCP was synthetized by a wet neutralization reaction using CaO (Merck, Germany) and H_3PO_4 (Merck, Germany), following the method described by Carrodegüas et al. [17].

For the preparation of the CPCs, MCPM (Merck, Germany) and *β*-TCP were mixed in the solid phase and, depending on the experiment, 1 % collagen (type I collagen fibers from bovine Achilles tendon, commercial grade, Brazil), as reinforcement and 1 % tetracycline (Ningxia Qiyuan Pharmaceutical Co., China), as antibiotic, to determine their possible use as a drug release system, were added. A solution of 0.1 % citric acid (Merck, Germany) was used as a liquid phase of the cements and as a setting retarder. A comparative study to analyse the composition effect on compressive strength, drug release and antimicrobial activity was carried out. The effect of the independent variables, the quantity of *β*-TCP used and the addition or not of collagen and/or tetracycline, was studied through the experiments described in Table 1.

Table 1. Experimental design. Liquid phase = 0.35 ml g^{-1}.

Series	MCPM (%)	*β*-TCP (%)	Collagen (%)	Tetracycline (%)
M(1)	48	50	1	**1**
M(2)	49	50	1	**–**
M(3)	49	50	–	**1**
M(4)	43	55	1	**1**
M(5)	44	55	1	**–**
M(6)	**44**	**55**	**–**	**1**

X-ray diffraction (XRD)

Phase characterization was carried out by means of X-ray diffraction, in a Philips, PW 1710 diffractometer (UK) with Cu-Ka radiation (k = 1.54056 nm) and Ni filter. The scan were made in a 2h angular interval of 10 – 60° and scanning speed of 18 min^{-1}. The results were interpreted using the X'Pert HighScore PANalytical program database, version 2.0.

Fourier transform infrared spectroscopy (FTIR)

Infrared spectra were obtained in a Fourier transform infrared spectrometer Shimadzu IR Tracer 100 (Japan), with a resolution of 4 cm^{-1} and 21 scans per sample in a range of 400-4 000 cm^{-1}.

Scanning electronic microscopy (SEM)

The samples were coated with a 20 nm film of gold in a BAL-TEC MED 020 system and placed in a desiccator until analysis. A JEOL microscope, JSM-6360LV with Oxford EDX probe (USA), magnification of 5 – 300000, resolution of 3 nm and acceleration voltage of 20 kV, was used for the microstructural analysis.

Mechanical characterization

For the compressive strength of the material, 12 mm height and 6 mm diameter specimens were prepared. The samples were immersed in Ringer's solution at 37 °C and tested, after 24 h of the cement preparation, immediately after being extracted to maintain hydration. The study was carried out in a universal testing machine with load cell of 200 N and at 1 mm min^{-1} load application speed. The compressive strength (r_c) in MPa was determined by the following formula:

$$\sigma_c = \frac{F}{A_0} = \frac{4P}{\pi d^2} \cdot 10^{-6} \qquad (1)$$

where *P* is the maximum breaking load (N) and *d* the diameter of the specimen (m). Five specimens were tested for each formulation.

Drug release study

Test specimens of the cements of 6 mm in height and 12 mm in diameter loaded with tetracycline were used. The samples were immersed in 10 mL of Ringer's solution in glass bottles at (37.0 ± 0.5) °C throughout the study. The solution in contact with the specimens was completely extracted at the established times and replaced with 10 mL of fresh solution. The extractions were made every half hour until 5 h of the cement preparation and, after that, at 24 h up to seven days. Five specimen of each formulation were prepared and evaluated. The determination of the antibiotic released to the solution was carried out in a UV-Visible Spectrophotometer (Shimadzu,

Japan) at a wavelength of 276 nm; and the results were reported as a cumulative amount of the tetracycline released versus time [18].

Microbiological study

For the microbiological study, specimens of 6 mm in height and 12 mm in diameter were prepared. In order to evaluate the antimicrobial susceptibility of the composites, strains of *Escherichia coli* ATCC 10536 were used, at a strain concentration adjusted with a turbidimetric method employing as a reference a 0.5 MacFarland standard ($1 \cdot 10^8$ CFU mL^{-1}).

Subsequently, 500 μL of a previously prepared culture medium of Mueller-Hinton agar (Merck) was inoculated in Petri dishes. After a period of 20 min the test specimens were placed on top of the plates containing the culture medium and the bacterial suspension and were incubated at 37 ± 1 °C for a period of 72 h. Three specimens were tested for each formulation and the inhibition zone was measured with the software SCAN 500 Automatic Colony Counter Version 6.

Statistical calculations

Graphs, statistics and mathematical calculation of nonlinear models to evaluate release mechanisms were performed with OriginPro 2016.

Results and discussion

Once the cements were prepared, a malleable paste that set in about 2 to 3 min was obtained. The setting time delay regarding the values reported for brushite cements of less than 30 s [4, 19] was achieved with the addition of 0.1 % of citric acid to the liquid phase used as a reaction retarder [20]. The accepted mechanism for the setting reaction of the cement paste goes through the dissolution of the components, the formation of a gel and the nucleation and growth of brushite crystals, according to the reactions described in Eqs. (2 – 4) [4]. During the initial dissolution of MCPM a considerable decrease in pH occurred, followed by an increase during the dissolution of b-TCP due to the exposure to an acid environment. Finally, the precipitation and growth of interlocked brushite crystals resulted in a solid material. Equation (5) describes the complete setting reaction of the brushite cements.

$$Ca(H_2PO_4)_2 \bullet H_2O = Ca^{2+} + 2H_2PO_4^- + H_2O \quad (2)$$

$$\beta\text{-}Ca_3(PO_4)_2 + 4H^+ = 3Ca^{2+} + 2H_2PO_4^- \quad (3)$$

$$Ca^{2+} + H_2PO_4^- + 2H_2O = CaHPO_4 \bullet 2H_2O + H^+ \quad (4)$$

$$\beta\text{-}Ca_3(PO_4)_2 + Ca(H_2PO_4)_2 \bullet H_2O + 7H_2O = 4CaHPO_4 \bullet 2H_2O \quad (5)$$

Since, in aqueous solutions at physiological *pH*, DCPD is known as a precursor of hydroxyapatite that is more thermodynamically stable, the transformation of the cements once implanted should be expected. This transformation occurs through a dissolution–reprecipitation mechanism. Due to the relatively low solubility of brushite in water the presence of Ca^{2+} ions in the medium is needed to trigger the reprecipitation process [21], which occurs according to the following reaction (Eq. (6)) thanks to the Ca ions present in the body fluids.

$$CaHPO_4 \bullet 2H_2O + (3\text{-}x)Ca_3(PO_4)_2 = Ca_{10\text{-}x}(PO_4)_{6\text{-}x}(OH)_2 + H_3PO_4 \quad (6)$$

XRD and FTIR

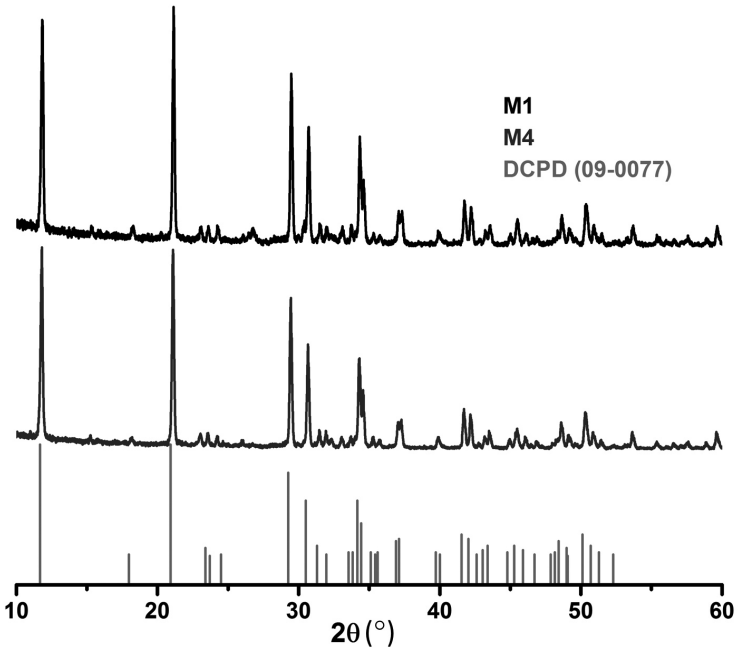

Figure 1. XRD pattern of samples M1 and M4, all the peaks corresponds to DCPD according to the ICDD PDF 9-0077 X-ray diffraction pattern. The maximum intensity DCPD peaks could be observed at 2h = 11.681° and 20.935°.

Figure 1 shows the DRX pattern of the cements samples M1 and M4 after 72 h of immersion in Ringer's solution. The most significant peaks of the pattern were compared with the ICDD PDF 9-0077 X-ray diffraction pattern of DCPD, which is the expected product of the setting reaction of the cement. A coincidence, in both, position and in intensity was observed, which confirms the occurrence of the setting reaction and the precipitation of brushite crystals. The results were very similar in all cements studied.

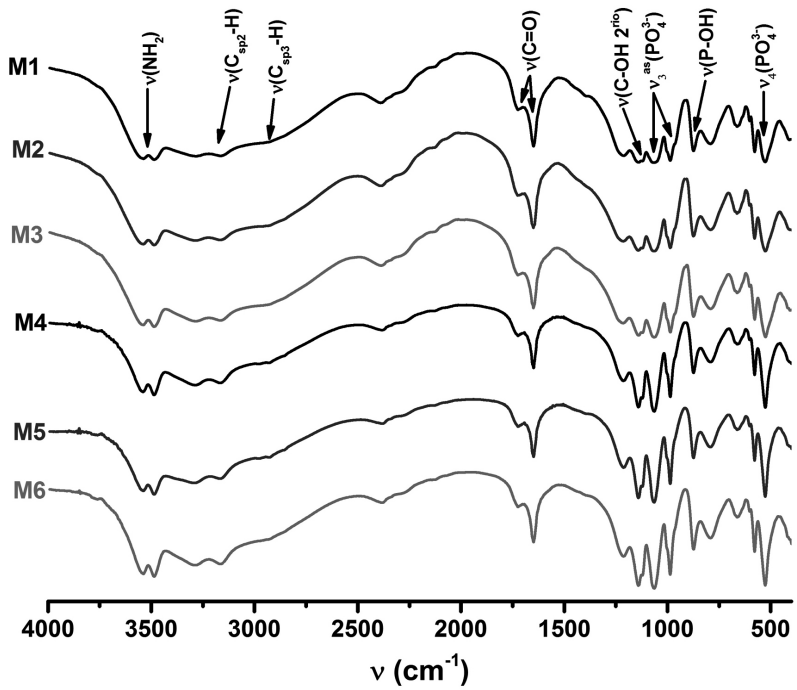

Figure 2. IR spectra of the samples

Figure 2 shows the FTIR spectra of the cements. The characteristic bands associated with the functional groups of calcium phosphates $\nu_3(PO_4^{3-})$ and the double signal of $\nu_4(PO_4^{3-})$ can be observed at 1119–1046, 605 and 570 cm^{-1} respectively In addition, some of the most relevant bands of the organic components, collagen and/or tetracycline, present in each formulation of the cements can be appreciated. Among them, the collagen bands corresponding to ν(C=O) and $\nu(Csp_3–H)$ at 1632 and 2 932 cm^{-1} can be identified. In the case of tetracycline, the ν(C=O), $\nu(Csp_2–H)$ and $\nu(NH_2)$ at 1 720, 3 148 and 3 280 cm^{-1}, respectively, can be observed. The spectra are very similar in all cases since the main component of the cement was the brushite obtained as a final setting reaction product, as discussed previously.

SEM

The morphology of the samples is shown in Figure 3. The presence of small pores of about 5 – 20 *μ*m can be seen; the samples with collagen (M1, M2, M4 and M5) showed the smallest size of the pores due to the more compact structure achieved with the presence of collagen and the swelling of its fibers by the absorption of water. In addition, in the samples with collagen the fibers can be observed and distinguished as flatter and more uniform areas than the rest of the crystalline framework of the cement, which is not observed in the samples without collagen (M3, M6). The decrease in the size of the pores in the samples with the presence of collagen and the integration of the fibers of this compound in the crystalline framework of the cement influence the mechanical properties.

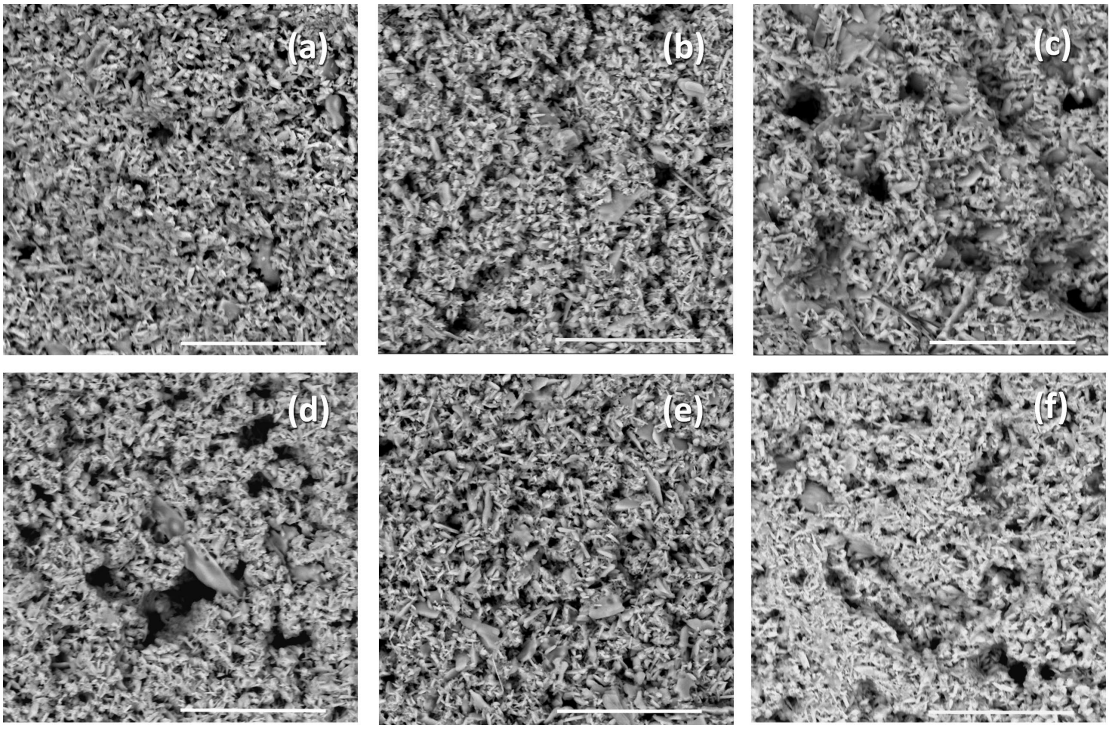

Figure 3. SEM micrographs of: (a) Cement M1, (b) Cement M2, (c) Cement M3, (d) Cement M4, (e) Cement M5, (f) Cement M6 (scale bar = 50 µm). Samples M1, M2 and M3 contain less β-TCP compared to M4, M5 and M6, respectively. M1, M2, M4 and M5 contain collagen.

Compressive strength

Table 2 shows the results of the evaluation of the mechanical properties. The values of the compressive strength of the samples vary between 0.8 and 1.7 MPa, similar values are reported in the literature for other brushite cements [10, 22]. It is also observed that the specimens that present tetracycline and collagen in their formulations, M1 and M4, reached the highest values, followed by those that contain collagen in the formulation (M2 and M5). As expected, the addition of collagen enhances the mechanical properties, this result corresponds to the effect reported in other investigations [4, 13].

Table 2. Compressive strength of the samples.

Samples	Compressive strength of the samples (MPa)
M1	1.7 ± 0.1
M2	1.3 ± 0.3
M3	1.0 ± 0.1
M4	1.4 ± 0.2
M5	0.9 ± 0.2
M6	0.8 ± 0.3

Drug release study

Normally when the release of drugs from biomaterials is studied, the interactions of the drug with the matrix must be taken into account, considering the molar mass of the active principle, its solubility, concentration and the porosity and mechanical properties of the support matrix.

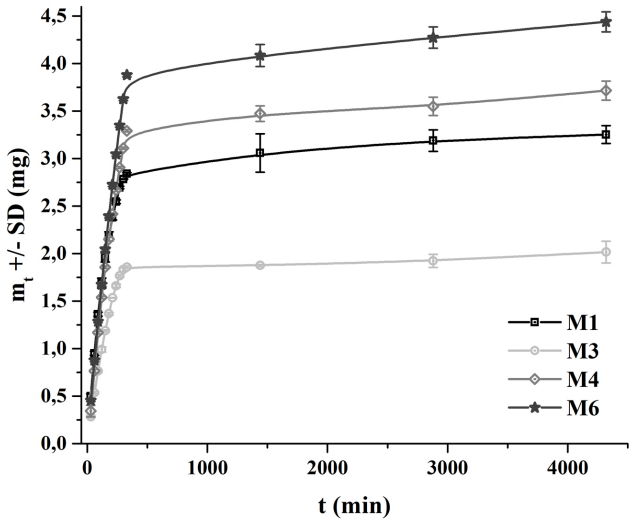

Figure 4. Release profiles of tetracycline. Samples M3 and M4 contain collagen. Samples M4 and M6 contain higher quantities of β-TCP compared to M1 and M3, respectively.

As it can be seen in Figure 4 the sample that released the most was M6, which did not contain collagen but had a higher proportion of *β*-TCP that did not react completely during the setting. When large quantities of *β*-TCP are used, part of it does not form a chemical bond with the crystalline framework and remains among the crystals; considering that this is one of the most soluble calcium phosphates, once in contact with an aqueous medium some gaps may be formed where *β* -TCP particles dissolve increasing the porosity of the cement. The liquid, Ringer's solution in this case, then penetrates easier into the material and extracts the drug. Therefore, when a higher proportion of this compound is introduced into the cement, more gaps are created, which enable the penetration of the liquid and therefore the release of the drug. In the case of samples containing natural polymer (M1 and M4), the material behaves more like a hydrogel that has the capability of retaining the liquid in its structure and regulates the release, therefore samples with collagen present a similar behaviour. However, once again the sample M4, which contains a greater quantity of *β*-TCP, is the one with the highest release because the increase in the porosity created by the *β*-TCP facilitates the drug release.

Calcium phosphate cement's capacity as controlled release systems has been reported to be dependent on diffusion during the first stages in accordance with the amount of drug on the surface layers of the matrices. However, as the study proceeds, the remaining tetracycline in the matrix is found in the most inaccessible areas of the fluid and the release mechanism must involve other processes besides the diffusion to allow the release of the drug.

The release mechanism of the drug of the formulations was studied through a series of mathematical models reported in the literature; the results obtained in the evaluation of the experimental data had a better fit to the logistic curve.

The generalized logistic function or curve, also known as the Richard curve, is a mathematical function that appears in various models of population growth, spread of epidemic diseases and dissemination in social networks. This function constitutes an extension of the sigmoid function for the growth of one magnitude [22], and is considered one of the best options to adjust dissolution curves [23].

The pharmacological variant, given by Eq. (8), was used:

$$Y = A2 + \frac{A1-A2}{1+\left(\frac{x}{x_0}\right)^p} \quad (8)$$

where *Y* is the amount of tetracycline released, *x* is time in minutes, *A*1 is the lower asymptote, *A*2 is the upper asymptote, x_0 is the value of the central node and *p* is the growth rate. Other interpretations, according to Adams et al. [23], lead to the Eq. (9):

$$X(t) = \frac{\alpha}{1+exp[(\beta-t)/\gamma]} \quad (9)$$

*A*1 – *A*2 is considered the *maximum* release percentage (α), β – *t* is *x* being β the time value for α/2, c is the time scale parameter which represents the distance between b and the point where the answer is $\alpha/(1 + e^{-1}) \approx 0.73\alpha$, equivalent to x_0. In this equation, Adams assumes the relationships of time and parameters as the argument of an exponential, while in the classical logistic equation used in our study the *p*-factor is the power, and the time relationships are then the basis of that power. The change in the magnitudes of the values from the mathematical point of view result in a change of the meaning of the parameters from the physical point of view in the pharmacokinetic phenomenon.

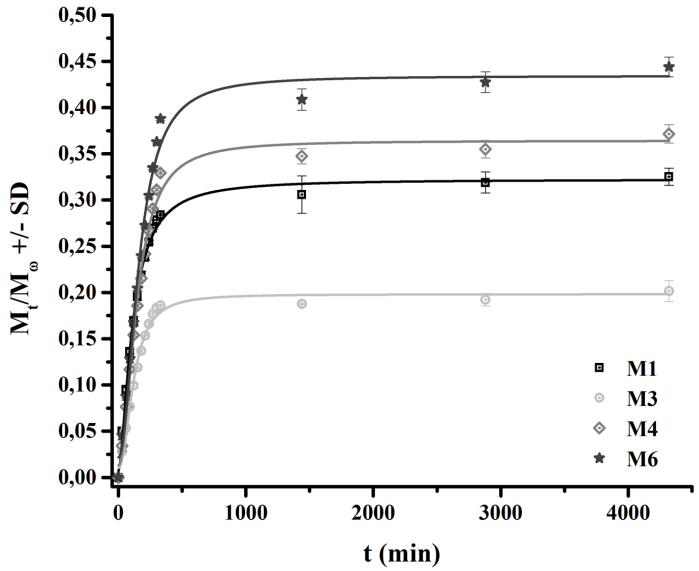

Figure 5. Adjustment to the logistic curve of the release profiles of the tetracycline.

Figure 5 shows the adjustment to the logistic curve of the release profiles. Coefficients of determination greater than 98 % were obtained, which confirms that this model represents the release process with accuracy. The values of the parameters for each sample are given in Table 3. The lower asymptote (*A*1) has values very close to zero, in the case of the superior asymptote (*A*2) the values obtained correspond to the maximum percentage of drug released by each sample. In addition, the values of *p* for each sample are approximately 2.

Table 3. Values of the parameters of the logistic curve for each sample.

Samples	*A*1	*A*2	x_0	*p*	χ^2_{red}	Adj. *R*-Square (%)
M1	0.007 ± 0.007	0.322 ± 0.004	111 ± 5	1.63 ± 0.09	5.310^{-5}	99.47
M3	0.011 ± 0.006	0.198 ± 0.004	120 ± 7	2.1 ± 0.2	6.210^{-5}	98.54
M4	0.013 ± 0.009	0.364 ± 0.007	145 ± 7	2.0 ± 0.2	1.510^{-4}	98.95
M6	0.02 ± 0.01	0.43 ± 0.01	159 ± 9	2.1 ± 0.2	2.910^{-4}	98.59

It can be concluded that the release of tetracycline from the matrices is governed by a mechanism of diffusion in the first hours, mainly due to the drug that is close to the edges of the matrix according to the geometric shape of matrices and the drug solubility. At the second stage, the release not only depends on the solubility of the drug, but also on other mechanisms such as the advance of the release front, the concentration of the drug and the diffusion medium. In this case, the logistic function that fits the release profiles manages to encompass not only the mechanisms of the second stage but also the diffusive mechanisms that govern the first stage, which is why it is able to describe the entire release process.

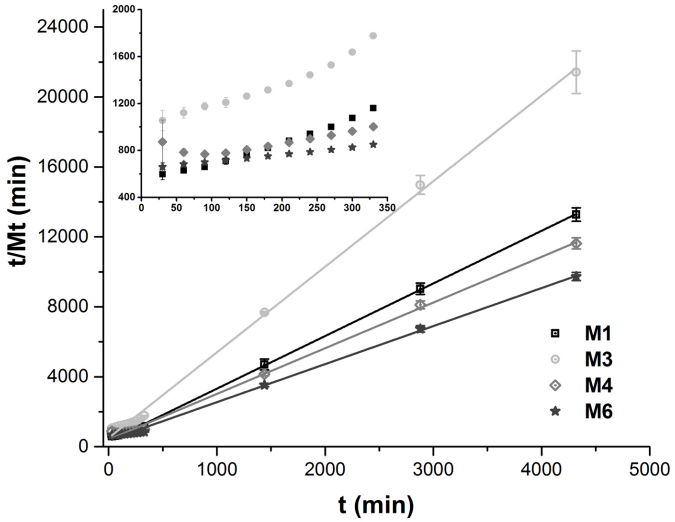

Figure 6. Prediction of the total drug release (M∞).

Another important analysis is the prediction of the total tetracycline released by the sample in an infinite time. For this purpose, the following equation was used:

$$\frac{t}{M_t} = \frac{1}{M_\infty} t + \frac{1}{k_{lib} M_\infty^2} \quad (10)$$

where t is time, M_t is the amount of drug released in time, M_∞ is the final amount of sample released for an infinite time and k_{lib} represents the kinetic constant of release [24]. The results of this analysis are shown in Figure 6 where the adjustment to the equation is observed, and the behaviour in early times (first day) can be seen in the inset. The differences in final tendencies of the sample release capacity are already appreciated after the first four hours; nonetheless, before that time, the samples present almost the same behaviour because the first stage is dependent solely on diffusion and the drug is equally homogeneously distributed on the surface of all samples due to the preparation method. When the release front advances, then it becomes more dependent on the actual composition of the cement and the characteristics arising from the release process such as increased porosity and pore size, the biodegradability of the material and presence of collagen.

Table 4 shows the comparison between the maximum values of release during the study ($A2$) and M_∞, which represents the prediction of the total drug released. The total release values indicate that the sample M6, which exhibited the best performance on release during the study, would be the one that releases the most, 46.0 %. It also, establishes that M3 with only 20.4 % would be the lowest release. In addition, it should be noted that this equation presents an adjustment of more than 99 % to the profiles obtained in the study.

Table 4. Prediction values of M_∞.

Samples	slope	*A2*	M_∞.	R^2 (%)
M1	3.01 ± 0.02	0.322 ± 0.004	0.332 ± 0.003	99.92
M3	4.89 ± 0.06	0.198 ± 0.004	0.204 ± 0.003	99.80
M4	2.61 ± 0.04	0.364 ± 0.007	0.383 ± 0.006	99.68
M6	2.18 ± 0.03	0.430 ± 0.01	0.460 ± 0.007	99.73

Microbiological study

Table 5 shows the final diameters of the inhibition growth halos within 72 h, where there was no bacterial growth due to the release of the drug to the culture medium. The behavior of inhibition on the *Escherichia coli* culture whit time is shown in Figure 7 by the measurements of the halos' diameters at 24, 48 and 72 h. In all cases, the tetracycline effect on the culture can be observed by the inhibition halo, ensuring that the drug preserved the biological activity after the setting of the different compositions cements. The sample with the largest inhibition halo (M6) correspond to the one with highest release of the drug, as expected.

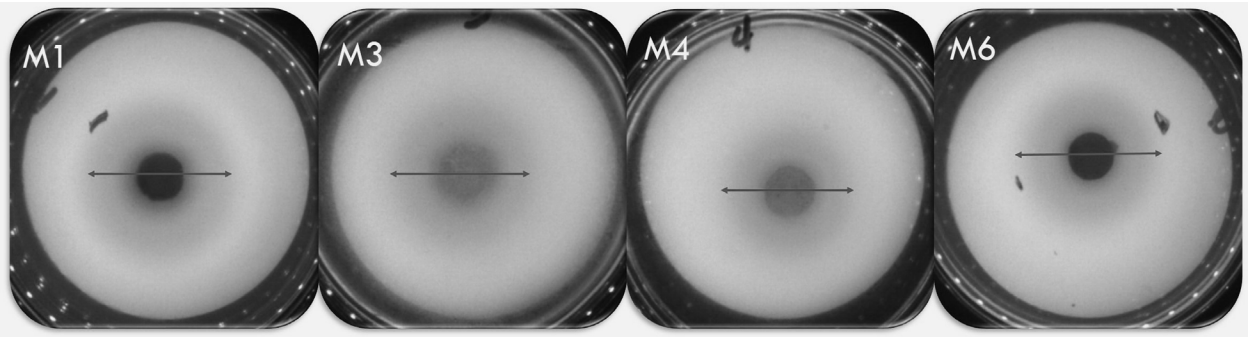

Figure 7. Final diameters of the inhibition halos at 72 h. From left to right, samples M1, M3, M4 and M6 (mm).

Table 5. Diameter of the inhibition growth halos on time.

Time (h)	inhibition halo diameter (mm)			
	M1	M3	M4	**M6**
24	16.3 ± 0.2	13.4 ± 0.2	13.9 ± 0.2	14.2 ± 0.2
48	29.9 ± 0.3	28.9 ± 0.1	27.7 ± 0.2	32.2 ± 0.3
72	43.3 ± 0.2	41.5 ± 0.3	40.1 ± 0.3	47.7± 0.3

Conclusions

Six formulations of a DCPD were prepared, in which a malleable paste that set after about 2 or 3 min was obtained. The addition of collagen was the most relevant variable on the increase of the compressive strength of the samples, which varies between 0.8 and 1.7 MPa, values that allow their application in small maxillofacial defects.

The drug release profiles of tetracycline from the different formulations can be described by the logistic curve and is governed by a mechanism of diffusion in the first hours, while the advance of the release front, which depends on the composition, is more relevant in the second stage. The incorporation of a greater proportion of *β*-TCP increases the release of the tetracycline. The microbiological evaluation of the cements showed their effective antimicrobial activity against strains of *Escherichia coli* in a period of 24 to 72 h.

The proposed CPC is suitable for use as a drug delivery system with bone regenerative capabilities. In addition, the study of the drug release allowed the understanding of the mechanisms of the release phenomenon and could be used to predict the overall release behaviour in a complex CPC matrix with polymeric reinforcement.

References

[1] Dorozhkin, S. V. (2013). Calcium orthophosphate-based bioceramics. Materials, 6(9), 3840-3942.

[2] Dorozhkin, S. V. (2013). Self-setting calcium orthophosphate formulations. Journal of functional biomaterials, 4(4), 209-311.

[3] JZhang, J., Liu, W., Schnitzler, V., Tancret, F., & Bouler, J. M. (2014). Calcium phosphate cements for bone substitution: chemistry, handling and mechanical properties. Acta biomaterialia, 10(3), 1035-1049.

[4] Tamimi, F., Sheikh, Z., & Barralet, J. (2012). Dicalcium phosphate cements: Brushite and monetite. Acta biomaterialia, 8(2), 474-487.

[5] Sheikh, Z., Abdallah, M. N., Hanafi, A. A., Misbahuddin, S., Rashid, H., & Glogauer, M. (2015). Mechanisms of in vivo degradation and resorption of calcium phosphate based biomaterials. Materials, 8(11), 7913-7925.

[6] Ko, C. L., Chen, J. C., Hung, C. C., Wang, J. C., Tien, Y. C., & Chen, W. C. (2014). Biphasic products of dicalcium phosphate-rich cement with injectability and nondispersibility. Materials Science and Engineering: C, 39, 40-46.

[7] Alge, D. L., Goebel, W. S., & Chu, T. M. G. (2012). In vitro degradation and cytocompatibility of dicalcium phosphate dihydrate cements prepared using the monocalcium phosphate monohydrate/hydroxyapatite system reveals rapid conversion to HA as a key mechanism. Journal of Biomedical Materials Research Part B: Applied Biomaterials, 100(3), 595-602.

[8] Ginebra, M. P., Canal, C., Espanol, M., Pastorino, D., & Montufar, E. B. (2012). Calcium phosphate cements as drug delivery materials. Advanced drug delivery reviews, 64(12), 1090-1110.

[9] Vorndran, E., Geffers, M., Ewald, A., Lemm, M., Nies, B., & Gbureck, U. (2013). Ready-to-use injectable calcium phosphate bone cement paste as drug carrier. Acta biomaterialia, 9(12), 9558-9567.

[10] Mirtchi, A. A., Lemaitre, J., & Terao, N. (1989). Calcium phosphate cements: study of the β-tricalcium phosphate—monocalcium phosphate system. Biomaterials, 10(7), 475-480.

[11] O'neill, R., McCarthy, H. O., Montufar, E. B., Ginebra, M. P., Wilson, D. I., Lennon, A., & Dunne, N. (2017). Critical review: Injectability of calcium phosphate pastes and cements. Acta biomaterialia, 50, 1-19.

[12] Engstrand, J., Persson, C., & Engqvist, H. (2014). The effect of composition on mechanical properties of brushite cements. Journal of the mechanical behavior of biomedical materials, 29, 81-90.

[13] O'Hara, R. M., Orr, J. F., Buchanan, F. J., Wilcox, R. K., Barton, D. C., & Dunne, N. J. (2012). Development of a bovine collagen–apatitic calcium phosphate cement for potential fracture treatment through vertebroplasty. Acta biomaterialia, 8(11), 4043-4052.

[14] Hong, Y. J., Chun, J. S., & Lee, W. K. (2011). Association of collagen with calcium phosphate promoted osteogenic responses of osteoblast-like MG63 cells. Colloids and Surfaces B: Biointerfaces, 83(2), 245-253.

[15] Bottino, M. C., Münchow, E. A., Albuquerque, M. T., Kamocki, K., Shahi, R., Gregory, R. L., ... & Pankajakshan, D. (2017). Tetracycline-incorporated polymer nanofibers as a potential dental implant surface modifier. Journal of Biomedical Materials Research Part B: Applied Biomaterials, 105(7), 2085-2092.

[16] Shahi, R. G., Albuquerque, M. T. P., Münchow, E. A., Blanchard, S. B., Gregory, R. L., & Bottino, M. C. (2017). Novel bioactive tetracycline-containing electrospun polymer fibers as a potential antibacterial dental implant coating. Odontology, 105, 354-363.

[17] García Carrodeguas, R., Morejón Alonso, L., García-Menocal, J. A. D., Morejón Alonso, L., Ginebra Molins, M. P., Martínez Manent, S., ... & Planell Estany, J. A. (2003). Hydrothermal method for preparing calcium phosphate monoliths. Materials Research, 6, 395-401.

[18] Peppas, N. A., & Narasimhan, B. (2014). Mathematical models in drug delivery: How modeling has shaped the way we design new drug delivery systems. Journal of Controlled Release, 190, 75-81.

[19] Mirtchi, A. A., Lemaître, J., & Hunting, E. (1989). Calcium phosphate cements: action of setting regulators on the properties of the β-tricalcium phosphate-monocalcium phosphate cements. Biomaterials, 10(9), 634-638.
[20] Barralet, J. E., Grover, L. M., & Gbureck, U. (2004). Ionic modification of calcium phosphate cement viscosity. Part II: hypodermic injection and strength improvement of brushite cement. Biomaterials, 25(11), 2197-2203.
[21] Cuneyt Tas, S.B. Bhaduri. Preparation of Brushite Powders and their in Vitro Conversion to Nanoapatites. In Bioceramics: Materials and Applications V. John Wiley & Sons (2012).
[22] Richards, F. J. (1959). A flexible growth function for empirical use. Journal of experimental Botany, 10(2), 290-301.
[23] Adams, E., Coomans, D., Smeyers-Verbeke, J., & Massart, D. L. (2002). Non-linear mixed effects models for the evaluation of dissolution profiles. International journal of pharmaceutics, 240(1-2), 37-53.
[24] Valles, E., Durando, D., Katime, I., Mendizábal, E., & Puig, J. E. (2000). Equilibrium swelling and mechanical properties of hydrogels of acrylamide and itaconic acid or its esters. Polymer bulletin, 44, 109-114.